CellPress
OPEN ACCESS

Trends in
Biotechnology

Research Article

Staying productive under pressure: systems evaluations of ß-carotene production in *Yarrowia lipolytica* under continuous fermentation

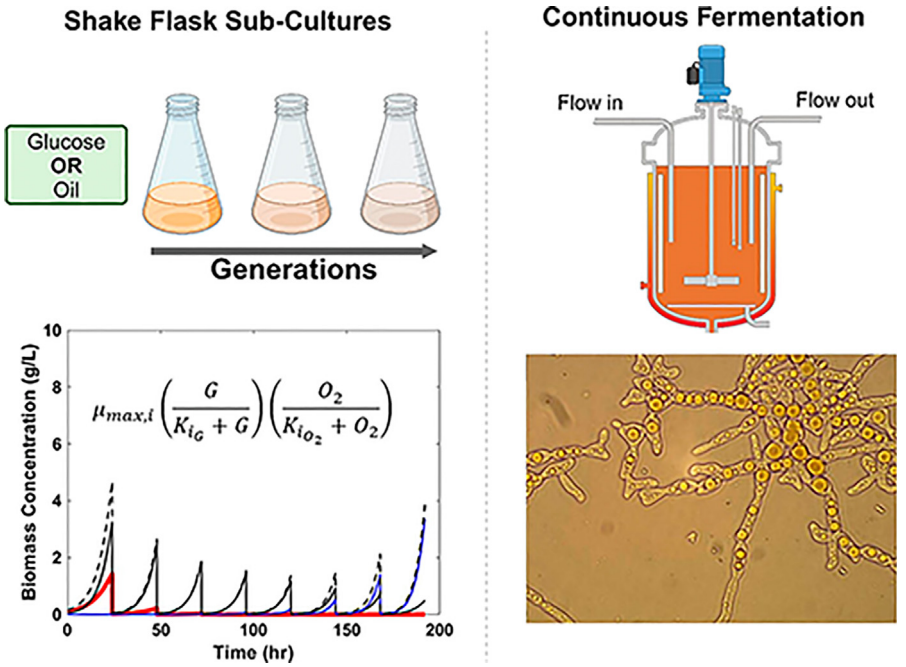

This integrative experimental and modeling study explores how fermentation conditions affect β-carotene production in *Yarrowia lipolytica*. Oil-based feedstocks enhance stability in continuous fermentation compared with glucose, while high-yielding laboratory strains often falter in industrial bioreactors, where faster-growing but less productive variants dominate under stress and determine long-term outcomes.

Alyssa M. Worland, Vincent A. Xu, Maria F. Duran, Philip Gitman, Kristen Hunter-Cevera, Cinzia Klemm, Yufei Sun, Diego Ruiz Sanchis, Rodrigo Ledesma-Amaro, Kyle R. Pomraning, Deepti Tanjore, Mark Blenner, Yinjie J. Tang

blenner@udel.edu (M. Blenner)
yinjie.tang@wustl.edu (Y.J. Tang).

Highlights

Different cultivation modes (batch, fed-batch, continuous) and culture conditions are tested to assess the long-term β-carotene production capacity of *Yarrowia lipolytica*.

Continuous fermentation hastens the emergence of low-producing subpopulations in engineered *Y. lipolytica*.

Oxygen limitation and high dilution rates in continuous bioreactors greatly reduce sustained β-carotene production.

Oil feedstock amplifies population heterogeneity but boosts β-carotene yield and stabilizes production.

Bioreactor kinetic models reveal subpopulation dynamics and offer mechanistic insights into observed experimental outcomes.

To reduce the risks of commercializing laboratory strains, scale-down approaches using continuous fermentation should be developed to assess their scalability.

Trends in Biotechnology, January 2026, Vol. 44, No. 1
https://doi.org/10.1016/j.tibtech.2025.08.019

Trends in Biotechnology

CellPress OPEN ACCESS

Research Article

Staying productive under pressure: systems evaluations of ß-carotene production in *Yarrowia lipolytica* under continuous fermentation

Alyssa M. Worland[1,2,3], Vincent A. Xu[1], Maria F. Duran[2], Philip Gitman[4], Kristen Hunter-Cevera[2,3], Cinzia Klemm[5], Yufei Sun[1], Diego Ruiz Sanchis[5], Rodrigo Ledesma-Amaro[5], Kyle R. Pomraning[3,6], Deepti Tanjore[2,3], Mark Blenner[4,*], and Yinjie J. Tang[1,*]

Scaling biomanufacturing from laboratory to industrial scale poses significant challenges, especially for continuous fermentation. This study investigates these challenges using a β-carotene-producing *Yarrowia lipolytica* strain. Through fermentation experiments and proteomics, we have assessed how fermentation modes, carbon sources, dissolved O_2, and media composition influence long-term bioproduction. In shaking flask subcultures, the strain maintained β-carotene production for over ~30 generations. However, in continuous fermentations, subpopulation shifted toward faster-growing low-producers, leading to significant production losses within just ~18 growth generations. This process was accelerated by O_2 limitation and high bioreactor dilution rates. Using canola oil as a carbon source increases population heterogeneity but enhances β-carotene biosynthesis and prolongs production compared with glucose-based media. Kinetic modeling suggests that strains optimized for the highest production in laboratory settings may be less robust in industrial environments, where suboptimal yet faster-growing variants gain a competitive edge under prolonged stress and ultimately shape overall continuous fermentation performance.

Introduction

The transition from laboratory to industrial-scale microbial biomanufacturing presents significant challenges. In controlled laboratory environments, microbial strains are often cultivated in shaking flasks, enabling consistent and predictable production yields. However, scaling up to industrial bioreactors introduces environmental heterogeneity and complexity. Factors such as imperfect mixing, oxygen variability, nutrient gradients, shear stress, and pH fluctuations create suboptimal growth conditions [1,2]. These stresses induce physiological changes in the microorganisms, reducing metabolic efficiency and, consequently, product yields [3]. Scale-up challenges are further compounded by the instability of synthetic biology strains, especially during the prolonged cell generations required for industrial fermentation [4]. The accumulation of genetic mutations during extended fermentations often leads to heterogeneous phenotypes, favoring less productive or nonproductive cell variants. However, **continuous fermentation** (see Glossary) offers great advantages for industrial manufacturing, such as lower capital investment, higher production rates, and better process optimization compared with batch or **fed-batch** cultures [5]. However, continuous fermentation poses challenges with engineered hosts, as the emergence of genetic or

Technology readiness

The production of carotenoids by engineered yeasts has been extensively studied under laboratory conditions. However, large-scale fermentation continues to face significant challenges due to genetic and nongenetic production losses. This study employs a scale-down fermentation approach to monitor β-carotene synthesis over multiple growth generations using an engineered industrial *Yarrowia lipolytica* strain in a fermentation environment relevant to industrial applications. The Technology Readiness Level of β-carotene fermentation currently ranges between 5 and 6. In this study, we conducted extensive experimental tests and kinetic simulations to evaluate β-carotene production during continuous fermentations. Key factors influencing fermentation stability include oxygen supply, shifts in cell population or strain composition caused by the washout effect, and substrate selection, such as the use of oil as the carbon source. Our simulations also suggest that suboptimal laboratory strains, characterized by relatively low production titers but faster growth rates, may have a better chance of maintaining production performance during scale-up and continuous fermentation processes. In conclusion, continuous fermentation not only offers the potential to boost productivity but also serves as a useful scale-down laboratory strategy for evaluating strain performance and understanding the interplay between metabolism, subpopulation dynamics, and bioprocess variables.

nongenetic subpopulations of low producers can lead to resource competition and productivity loss [6,7].

To better understand the drivers of productivity loss, this study employs a scale-down approach to examine titer instability in a β-carotene-producing *Yarrowia lipolytica* strain [4]. β-Carotene is an important metabolic intermediate for carotenoids and vitamin A production [8]. *Y. lipolytica* has gained attention as a promising chassis for the production of oleochemicals and terpenoids, owing to its natural abundance of acetyl-CoA [9]. It also exhibits robust growth on a wide range of carbon sources, including hydrophobic substrates, and demonstrates high chemical tolerance [10]. In this work, we characterize the phenotypic and production responses of the β-carotene-producing strain under various industrially relevant scale-down conditions. The study encompasses long-term (>10 days) fermentation conducted in three modes: continuous, semi-continuous, and shake flask sub-culturing (repeated batch). Key process variables, including oxygen limitation and carbon source, are systematically evaluated. Meanwhile, a kinetic model integrates subpopulation dynamics, mutation rates, and bioreactor conditions to explain their impact on bioproduction. By combining experimental observations with modeling, this study provides a framework to address critical questions about cellular heterogeneity and productivity loss. The insights gained bridge the gap between laboratory-scale performance and industrial realities, enabling targeted strategies for strain and bioprocess optimization.

[1]Department of Energy, Environmental and Chemical Engineering, Washington University in St. Louis, St. Louis, MO, 63130, USA
[2]Advanced Biofuels and Bioproducts Process Development Unit, Lawrence Berkeley National Laboratory, Emeryville, CA, 94608, USA
[3]US Department of Energy, Agile BioFoundry, Emeryville, CA, 94608, USA
[4]Department of Chemical and Biomolecular Engineering, University of Delaware, Newark, DE, 19713, USA
[5]Imperial College Centre for Synthetic Biology, Imperial College London, London, UK
[6]Chemical and Biological Processes Development Group, Pacific Northwest National Laboratory, Richland, WA, 99352, USA

*Correspondence:
blenner@udel.edu (M. Blenner) and
yinjie.tang@wustl.edu (Y.J. Tang).

Results

Comparison of fermentation modes on strain stability

For laboratory studies, shake flasks do not necessarily provide sufficient insight into strain behavior during industrial process scale-up [3,11]. The disparity arises from fundamental differences in the cultivation environments. In bioreactor conditions (e.g., continuous culture), cells and product are maintained at high level, leading to growth stresses and product inhibitions (Figure 1). By contrast, shake flask subculturing exposes cells to fresh media (biomass ranged from optical density $(OD)_{600}$ ~0.1–10), avoiding the accumulation of toxic products at high level. Further, the mixing dynamics of bioreactors can impose shear stress on cells. These dynamics can also create O_2 and nutrient gradients within industrial bioreactors [12,13]. Therefore, computational fluid dynamics (CFD) is used to illustrate complex microenvironments inside bioreactors [14,15].

In this work, β-carotene production was maintained for the most generations during shaking flask subculturing, with 50% titer loss not observed until ~30 generations in yeast extract peptone

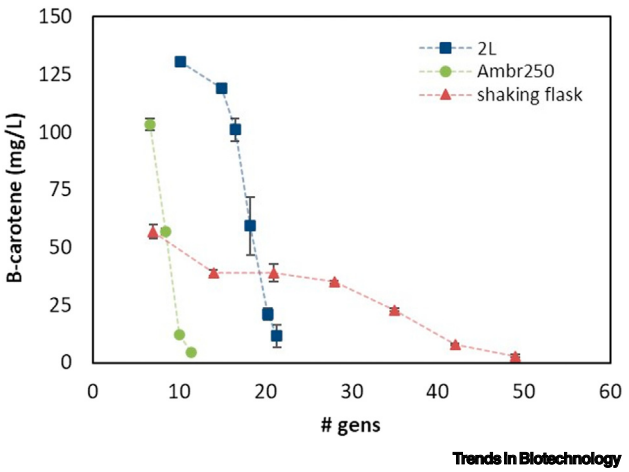

Figure 1. Impact of fermentation modes on production longevity. β-Carotene concentration (mg/l) after a given number of generations during cultivation in the three fermentation modes. Continuous fermentation in the 2l bioreactors is represented by blue markers, semi-continuous fermentation in Ambr250 bioreactors by green, and passaging in shaking flasks by red markers. Cells were cultivated in yeast extract peptone dextrose (YPD) media.

dextrose (YPD) cultures (Figure 1). Continuous and semi-continuous fermentations demonstrated lower titer stability. Continuous fermentations showed over 50% titer loss at ~18 generations, with over 90% loss observed at only ~21 generations. Interestingly, semi-continuous fermentation in **Ambr250** exhibited the greatest production losses of the three fermentation methods, with over 95% titer loss observed at ~11 generations. In flask cultures, the repeated subculturing may help maintain a higher proportion of high-producing cells with each passage, lending to the sustained production observed. Flask growth lacks the intense selection pressures of a continuous bioreactor, enabling a higher proportion of high producers to be maintained with each passage. Moreover, subculturing in shaking flasks offers an advantage by repeatedly exposing cells to fresh, nutrient-rich, inhibitor-free media. This periodic renewal of the growth environment contrasts with continuous bioreactor conditions, where cells face gradual accumulation of metabolic byproducts and debris (as shown in our previous shaking flask results [16]). In continuous operations, faster-growing, lower-producing variants outcompete high producers, a selection pressure intensified by the constant washout of producing cells. Moreover, the semi-continuous nature of the Ambr250 fermentation allows for accumulation of cellular products and wastes, exacerbating the loss of productivity. Besides, the smaller impellers in the Ambr250 system generate less mixing power compared with 2l bioreactor [17], which may limit O_2 transfer. These findings highlight the complex relationship between cultivation methods and strain stability, underscoring the need for a more nuanced approach to strain development and scale-up strategies.

Effect of carbon sources on production longevity

Y. lipolytica possesses a unique ability to efficiently catabolize various carbon sources, including unrefined oil feedstocks [10,16]. Previous studies have demonstrated the potential of *Y. lipolytica* in converting waste oils into high-value products such as length-modified fatty acids and citric acid [14,15,18–20]. Moreover, engineered terpene-producing strains of *Y. lipolytica* have shown increased terpenoid yields when cultivated with higher concentrations of oil feedstocks [21]. However, it remains unclear how oil feedstocks impact engineered strain (ES) stability during long duration bioreactor operations. Here, we evaluated titer stability during fermentation with canola oil as the carbon substrate. Our results revealed a striking difference in performance between canola oil and glucose-based media. We found that cells cultured in oil media exhibited significantly higher titers and a remarkably extended production compared with those grown in glucose-based media (Figure 2). We observed this across all three fermentation methods, suggesting a fundamental advantage conferred by oil substrates (Figure 3). During cultivation with oil, there is a marked increase in intracellular lipid body size (Figure 2B) [16]. Intracellular lipid bodies act as an *in vivo* extractive fermentation process sequestering the lipophilic β-carotene. This may help alleviate the metabolic stress of β-carotene accumulation within the cell; it may also reduce cell toxicity by decreasing the amount of β-carotene partitioning to the cell membrane [22–24]. Further, catabolism of fatty acids generates an abundance of acetyl-CoA, directing flux towards the tricarboxylic acid cycle (TCA) cycle and gluconeogenesis for energy generation, as well as towards the mevalonate pathway for β-carotene synthesis. The co-utilization of glycerol component of the oil substrate not only supports a balanced central metabolism and NADPH generation, but also reduces the loss of carbon as CO_2 [25]. Further, dissolved oxygen (DO) in plant oil is approximately five times higher than that in water at 30°C [26,27]; this effect could facilitate O_2 transfer in yeast, peptone, and oleic acid (YPO) fermentation (Figure 4). *Y. lipolytica*, being an oleaginous yeast, tends to flocculate around extracellular lipid droplets. Intracellular lipid accumulation can enhance O_2 transport across the phospholipid bilayer to the mitochondria in oil media. Studies have also demonstrated oxygen diffusion accelerated by cellular lipids [28]. A similar effect may occur in lipid fermentations, where hydrophobic channeling from the medium's lipid phase

Glossary

Ambr250: a bioreactor device used for fed-batch cultivation.
Continuous fermentation: cultivation mode where input streams (e.g., fresh media, etc.) are fed into the culture during cultivation, and output streams of culture material (including cell biomass, product, unused substrate, etc.) are removed from the culture during cultivation; the input and output streams are of the same flow rate.
Dilution rate: the input/output volumetric flow rate in a continuous bioreactor divided by the bioreactor volume.
Fed-batch: cultivation mode where input streams (e.g., fresh media, etc.) are fed into the culture during cultivation.
Growth-associated production: in this work, it is defined as the product formation that is directly proportional to producing biomass growth rate.
Metabolic burden: cellular resource demand caused by the existence of engineered pathways and bioproduction.
Non-growth-associated production: in this work, it is defined as the product formation that is directly proportional to producing biomass concentration, regardless of whether the cell doing the production is actively growing.

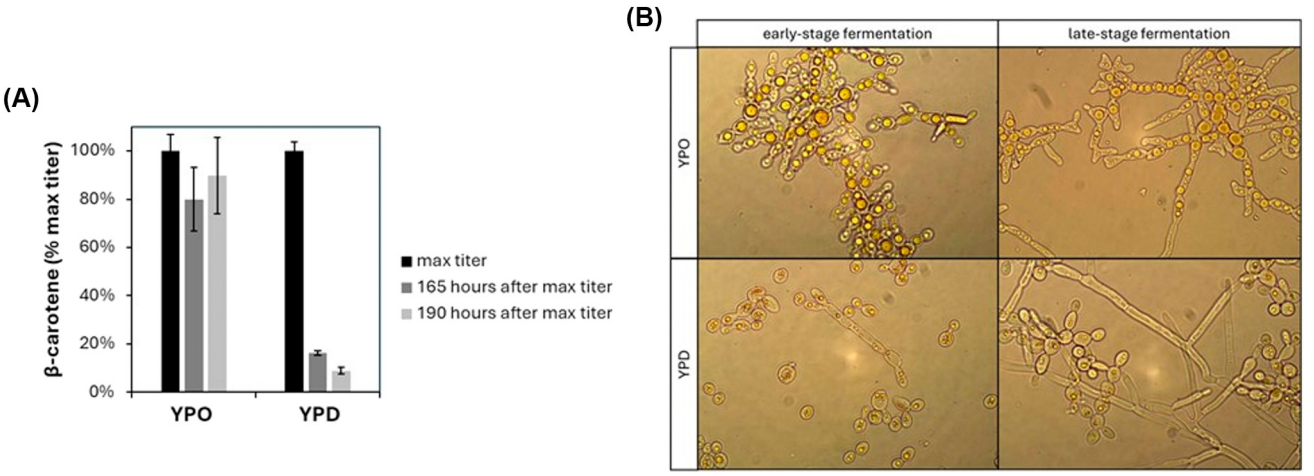

Figure 2. Continuous β-carotene fermentation with oil or glucose. (A) Bars represent titer as a percentage of the maximum titer reached during fermentation in oil-based (YPO) and glucose [yeast extract peptone dextrose (YPD)] media. The engineered strain has lost over 80% of production 165 h after maximum titer in YPD and nearly 90% of production is lost 190 h after maximum titer in YPD. However, during cultivation with oil, the strain retains 80% ± 13% of its production. (B) Images of intracellular lipid bodies and filamentation formation in continuous bioreactor cultures. Cells cultivated with oil media [yeast, peptone, and oleic acid (YPO)] at early- and late-stage fermentation exhibit larger lipid bodies and sustained production compared with cells cultured in glucose media at both early- and late-stage fermentation. Cell filamentation increases with cultivation time.

to cell membranes increases oxygen uptake rates. Collectively, these factors may enhance producer subpopulation and their biosynthetic pathways (Figure 5).

Y. lipolytica is a filamentous yeast and the transition from ovoid to filamentous forms can be induced by external environmental stressors (Figure S1 in the supplemental information online) [29,30]. Filamentous cell formation is a major drawback for industrial fermentation as the

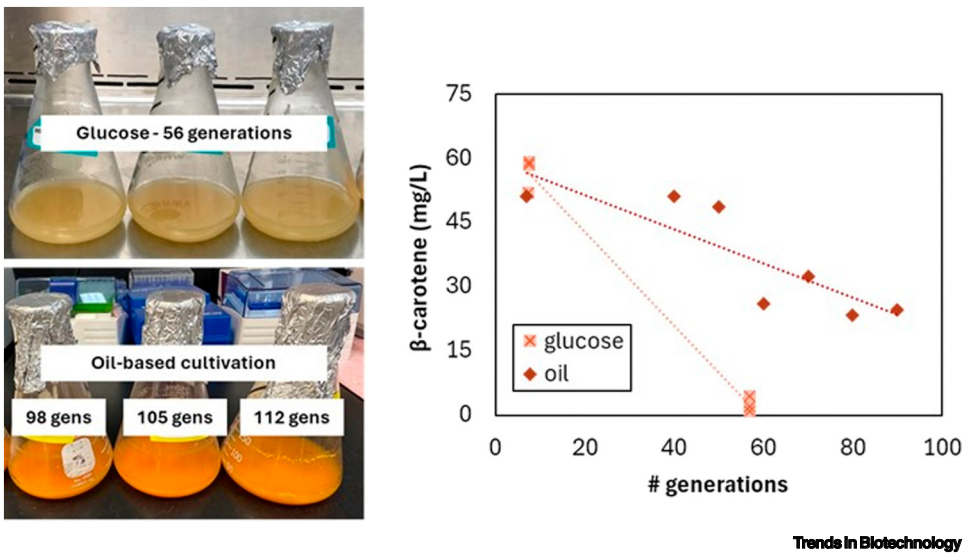

Figure 3. Titer stability of cells cultured with oil or glucose in shaking flasks. Oil media [yeast, peptone, and oleic acid (YPO)] contributes to a significant improvement in β-carotene titer stability, with only 40% of production loss observed after more than ~90 generations. Cultures grown in glucose [yeast extract peptone dextrose (YPD)] demonstrate over 90% production loss after only ~56 generations.

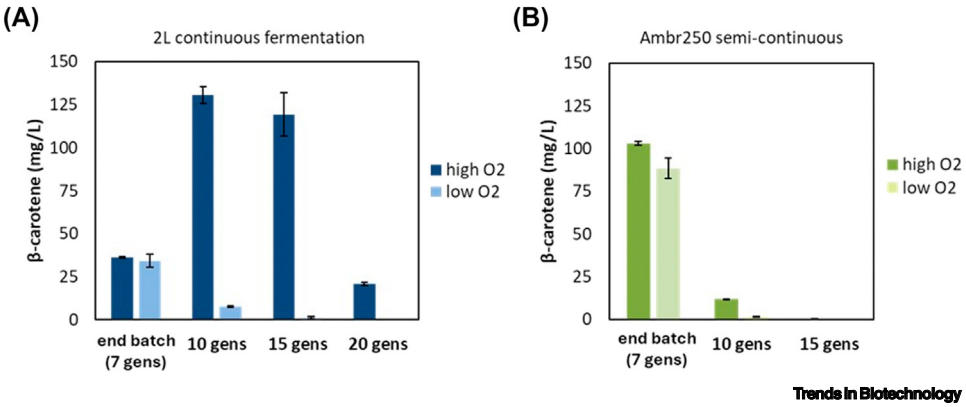

Figure 4. Impact of oxygen limitation on strain stability in yeast extract peptone dextrose (YPD) media. O_2 limitation causes an increased rate of titer loss during (A) 2l continuous fermentation and (B) Ambr250 semi-continuous fermentation. High and low oxygen supplementation is represented by dark- and light-colored bars, respectively. For all fermentations, the end of batch growth signifies the start of feed controls and induced oxygen limitation. All reactors were cultured at the same conditions during batch cultivation.

filamentous cells cause mixing inefficiencies, which can exacerbate cell stressors due to oxygen or nutrient depleted microenvironments within the bioreactor. In later stages of bioreactor fermentation, cell filamentation increases (Figures 2B and 5C). In glucose cultures, filamentation is correlated with decreased production (Figure 2B). Likely, this is due to cell energy being diverted towards biomass growth rather than synthesis of secondary metabolites. However, during fermentation in oil media, we observe that even though filamentation occurs to the same degree as glucose cultures [16], filamentous cells still produce β-carotene (Figure 2B and Figure S1).

Impact of aeration and nutrient composition

During fermentation scale-up, maintaining uniform O_2 and nutrient distribution becomes increasingly difficult as vessel size increases [31]. For example (Figure 4), we observed an increased rate of titer loss during both 2l continuous fermentation and Ambr250 semi-continuous fermentation under O_2-limited conditions. Insufficient aeration and mixing impair cell respiration and energy metabolism, inducing a strong selection pressure that prioritizes cell survival over product synthesis [32]. Media composition also plays a crucial role in strain stability. In nutrient-rich YPD medium, cells produce higher β-carotene titers compared with defined media [16]. By contrast, cultivation in yeast nitrogen base with amino acids (YNBaa) medium results in lower growth rates and overall β-carotene titers, likely due to the **metabolic burden** associated with both biomass synthesis and the expression of engineered pathways. For example, fermentation in the Ambr250 system showed that the defined medium led to lower productions than YPD medium, though specific productivity per unit biomass was comparable (Figure S2 in the supplemental information online). These results underscore the importance of optimizing bioreactor conditions and media compositions for industrial applications. In addition, media composition influences strain stability. In rich YPD media, cells achieve higher β-carotene titers compared with defined media [16]. This higher production is accompanied by a faster growth rate and a rapid loss of production overtime. By contrast, cultivation in defined YNBaa medium results in lower overall β-carotene titers but offers higher per-cell titers and a slower production decline rate. This finding underscores the critical role of media composition in fermentation performance and stability (Figure S2).

Cell population and proteomics analysis

Fluorescence microscopy has found that cellular β-carotene levels were heterogeneous during fermentation processes (Figure 5A). Due to the hydrophobic nature of β-carotene, accumulation

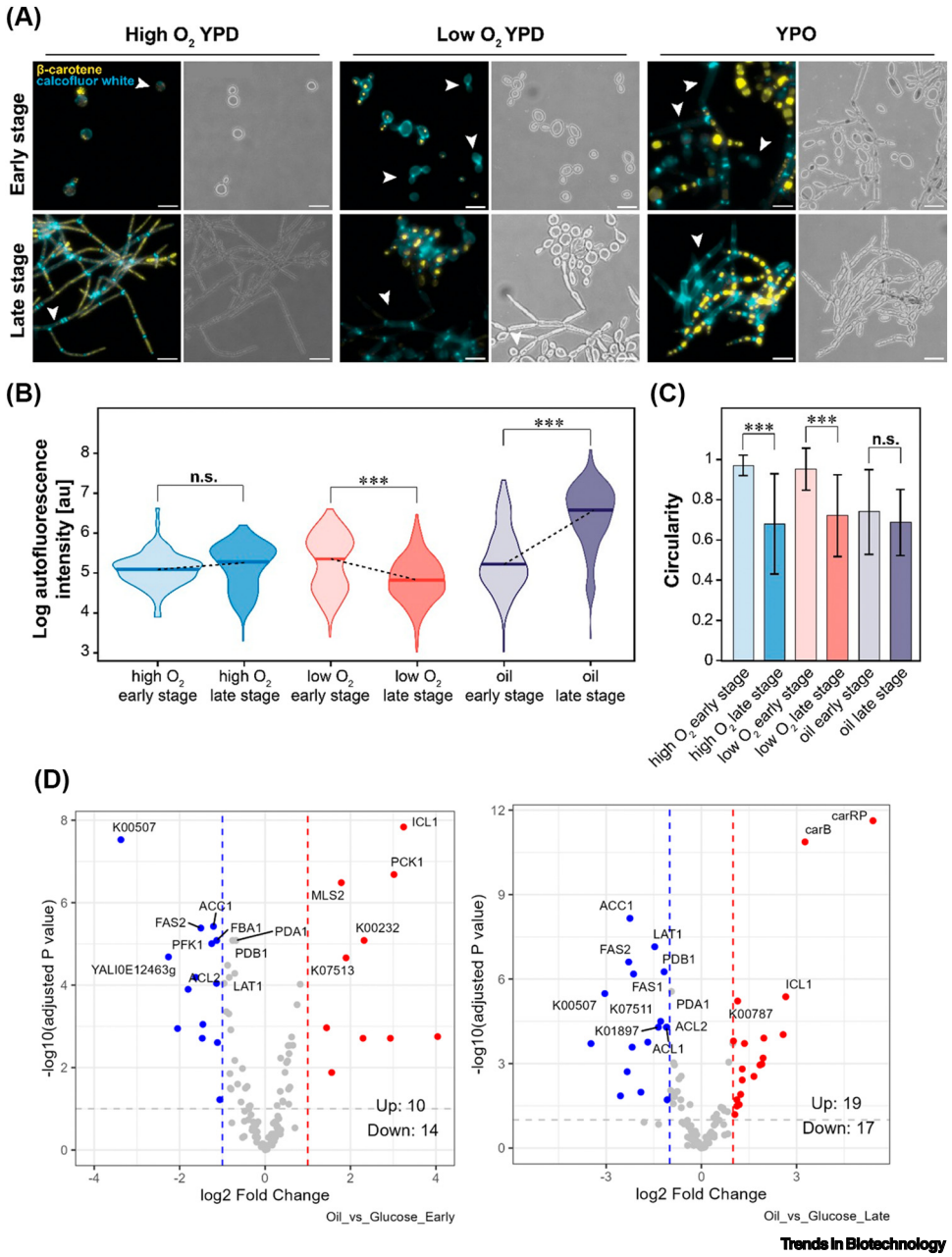

Figure 5. Cellular analysis of β-carotene production. (A) Representative micrographs showing β-carotene (yellow) within cells highlighted by calcofluor white cell wall staining. Images are taken from cells collected from early- and late-stage fermentation in low and high oxygen yeast extract peptone dextrose (YPD) and yeast, peptone, and oleic acid (YPO). White arrows highlight low producer cells. Scale bars are 10 μm. (B) Quantification of β-carotene fluorescence in different conditions and stages. Black broken lines indicate differences between mean intensities. High O_2 and low O_2 conditions are in YPD. YPO cultures are denoted as oil here. (C) Quantification of cell circularity based on area and perimeter of cells. High O_2 and low O_2 conditions are in YPD. YPO cultures are denoted as oil here. Significance was calculated using a student's *t*-test (n.s. = $P > 0.05$, *** = $P < 0.001$). (D) Analysis of protein expression fold changes in YPO media compared with YPD media. Volcano plot left: early fermentation stage. Volcano plot right: late fermentation stage.

is commonly observed in lipid bodies [33], producing distinct foci within cells. While even in early-stage fermentation at both high and low oxygen the number and intensity of fluorescent bodies were highly variable between cells, we noticed that during late-stage fermentation, high-producing populations were significantly decreased at low oxygen levels (Figure 5B), indicating that O_2 related stress leads to a selection pressure that favors low producer populations, which explains the drastic decrease of β-carotene titers over time (Figure 4). We observed that cells grown in YPO media contained much larger lipid bodies and that, while heterogeneity was present at both early- and late-stage fermentation, high-producers were maintained at a later stage (Figure 5B). Recent CFD studies have revealed that hydrophobic feedstocks significantly influence mixing conditions in *Y. lipolytica* fermentations, resulting in the formation of heterogeneous physical phases (hydrophobic, hydrophilic, and gaseous) [14,15,20,34]. Interestingly, these complex phase separations appear to enhance *Y. lipolytica* bioproduction and contribute to improved strain stability [15]. We also noticed that cells grown in YPO presented a reduced circularity during early-stage fermentation compared with cells grown in YPD, indicating an earlier onset of filamentation (Figure 5C). Filamentation was related to transcriptional reprogramming, lipid production, and remobilization [35]. We suspect that high lipid availability in YPO may lead to downregulated lipid remobilization. However, recent CFD studies have revealed that oil feedstocks greatly influence mixing conditions in *Y. lipolytica* fermentations [14,15,20,34], resulting in the formation of heterogeneous physical phases (hydrophobic, hydrophilic, and gaseous). Oil medium could not only increase O_2 transfer rates but also extract toxic fermentation products [21]. Proteomics analysis further revealed that

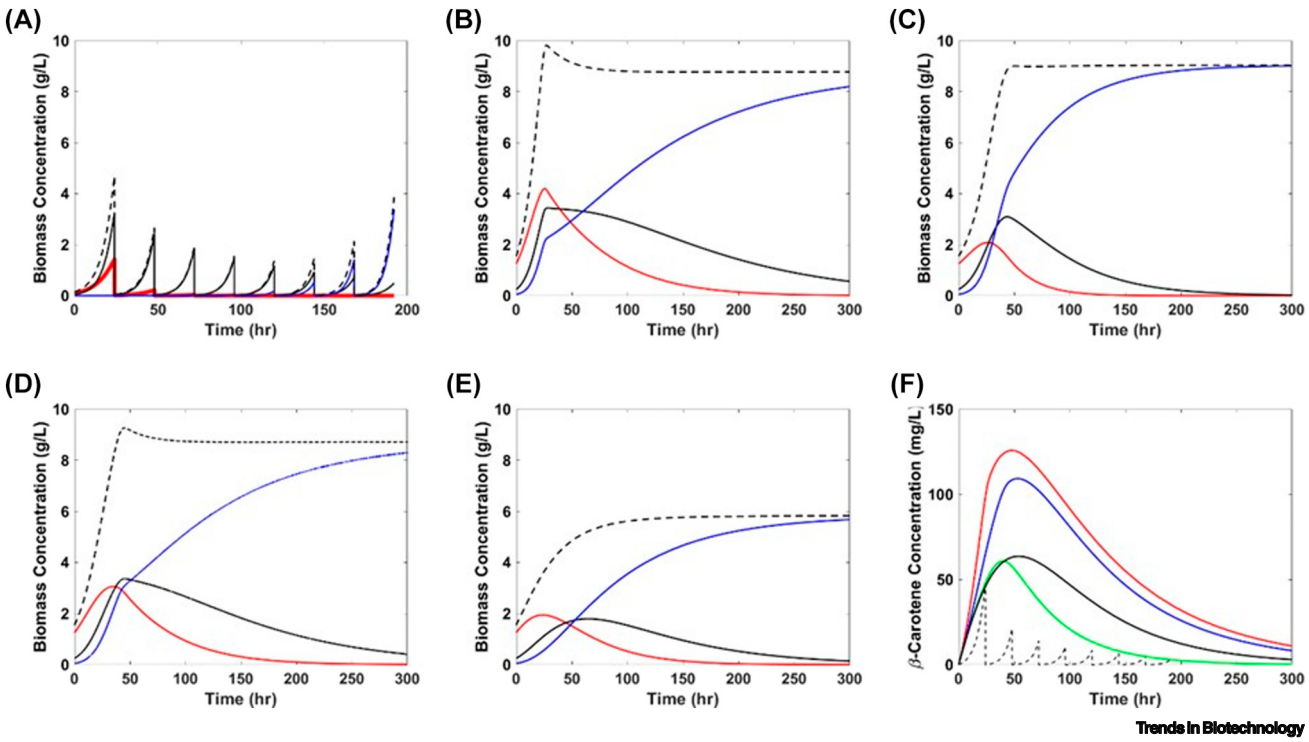

Figure 6. Simulation of cultivation mode, dilution rate, and dissolved oxygen (DO) effects on production performance. For biomass, red unbroken line: high-producing strain; black unbroken line: low-producing strain; blue unbroken line: non-producing strain; black broken line: total biomass. (A) Shaking flask passaging; each new batch starts with the previous batch's strain composition and 1% of the previous batch's end biomass concentration. Each batch is approximately seven generations. (B) Base case continuous culture with three distinct strains [non-producing (NP), low (LO), high (HI)]. (C) Continuous culture with three distinct strains, with a higher dilution rate of 0.08 h^{-1}. (D) Continuous culture with three distinct strains, with oscillating DO. (E) Continuous culture with three distinct strains and lower O_2 mass transfer coefficient (k_La reduced to 2 h^{-1}). (F) β-Carotene titer simulations. Black broken line : corresponds to Figure 6A; red unbroken line: corresponds to Figure 6B; green unbroken line : corresponds to Figure 6C; blue unbroken line : corresponds to Figure 6D; black unbroken line : corresponds to Figure 6E.

key β-carotene synthesis genes (CarRP and CarB) showed similar expression levels in YPO and YPD media at the start of fermentation but remained highly expressed in YPO during the late stage of continuous fermentation (Figure 5D). Notably, CarB encodes phytoene dehydrogenase, while CarRP encodes a bifunctional enzyme with lycopene cyclase and phytoene synthase activities.

Discussion

The β-carotene-producing ES exhibits heterogeneous phenotypes during cultivation. While high-producing cells are desirable, these cells have to compete with lower-producing, faster-growing cells [36]. Kinetic models were developed to aid our understanding of how population dynamics evolve over time, assessing the impact of numerous factors such as mutation rates and external selection pressures [37–39] (Figure 6, Tables S1 and S2 and Figures S3–S7 in the supplemental information online). Specifically, ES typically have slower growth rates than non-producing (NP) strains due to differences in metabolic burden. During fermentation, the high-producing strains are often outcompeted by low or NP strains. This effect is worsened by mutations or epigenetic changes induced by external stressors. Shaking flask passage enables higher specific growth rates and more generations per time than continuous culture (Figure 6A,B,F). Because of the

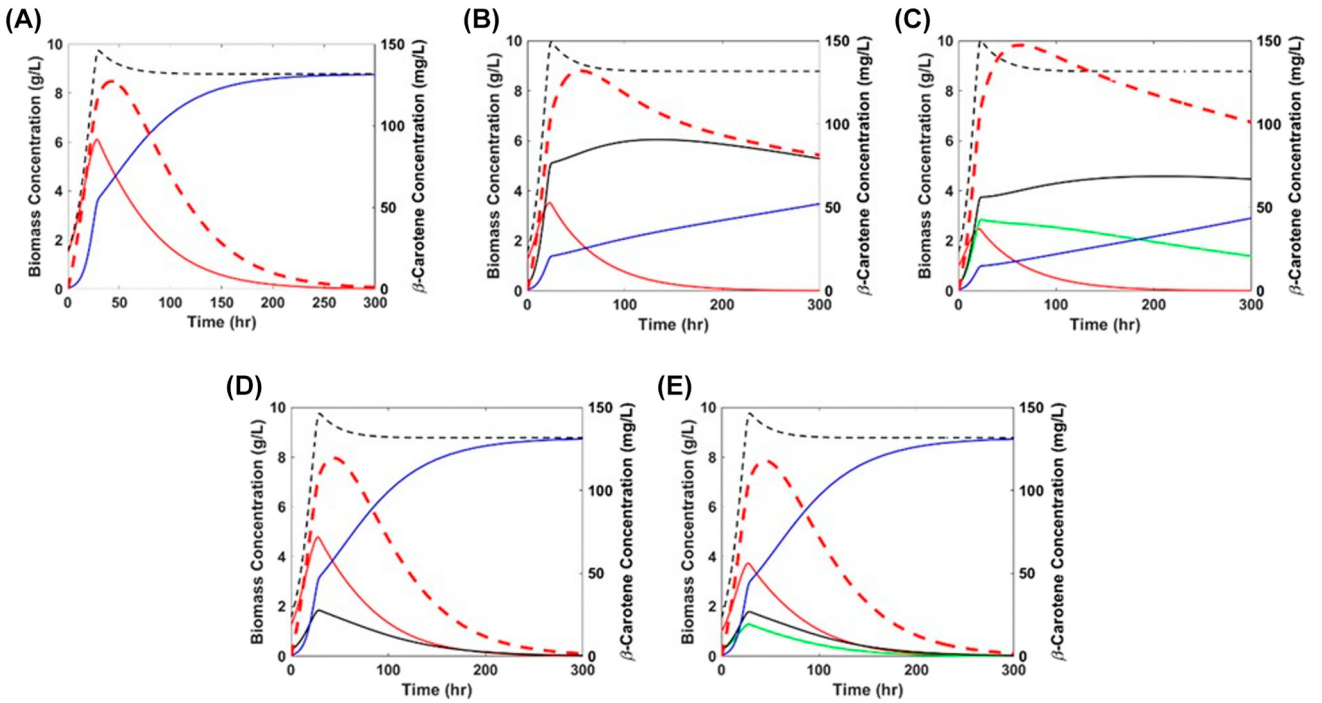

Figure 7. The effect of distribution of maximum specific growth rate ($\mu_{max,i}$) and half-saturation concentration of dissolved oxygen (DO) ($K_{i_{O_2}}$) of intermediate strains on production performance. Product yield (Y_{iP}) of all strains does not change from base case. Red unbroken line: high (HI); black unbroken line: low (LO); blue unbroken line : non-producing (NP); green unbroken line: medium (MED); black broken line : total biomass; red broken line : β-carotene. (A) Continuous culture with two distinct strains (NP and HI). (B) Continuous culture with three distinct strains (NP, LO, HI), with the $\mu_{max,i}$ and $K_{i_{O_2}}$ of intermediate strain (LO) clustering near $\mu_{max,NP}$ ($\mu_{max,LO} = 0.95\mu_{max,NP}$) and $K_{NP_{O2}}$ ($K_{LO_{O_2}} = \frac{K_{NP_{O_2}}}{0.95}$), respectively. (C) Continuous culture with four distinct strains (NP, LO, MED, HI), with the $\mu_{max,i}$ and $K_{i_{O_2}}$ of intermediate strains (LO, MED) clustering near $\mu_{max,NP}$ ($\mu_{max,LO} = 0.95\mu_{max,NP}, \mu_{max,MED} = 0.9\mu_{max,NP}$) and $K_{NP_{O2}}$ ($K_{LO_{O_2}} = \frac{K_{NP_{O_2}}}{0.95}, K_{MED_{O_2}} = \frac{K_{NP_{O_2}}}{0.9}$), respectively. (D) Continuous culture with three distinct strains (NP, LO, HI), with the $\mu_{max,i}$ and $K_{i_{O_2}}$ of intermediate strains (LO) clustering near $\mu_{max,HI}$ ($\mu_{max,LO} = 0.7\mu_{max,NP}$) and $K_{NP_{O2}}$ ($K_{LO_{O_2}} = \frac{K_{NP_{O_2}}}{0.7}$), respectively. (E) Continuous culture with four distinct strains (NP, LO, MED, HI), with the $\mu_{max,i}$ and $K_{i_{O_2}}$ of intermediate strains (LO, MED) clustering near $\mu_{max,HI}$ ($\mu_{max,LO} = 0.7\mu_{max,NP}, \mu_{max,MED} = 0.65\mu_{max,NP}$) and $K_{NP_{O2}}$ ($K_{LO_{O_2}} = \frac{K_{NP_{O_2}}}{0.7}, K_{MED_{O_2}} = \frac{K_{NP_{O_2}}}{0.65}$), respectively. Note: $\mu_{max,HI}$ and $K_{HI_{O_2}}$ values are held constant (see Table S1) in all scenarios shown in this figure.

repeated resetting of biomass concentration in shaking flasks, more generations occur per hour than in continuous cultures (Figure 1). In continuous cultivation, high-producing strains can be lost due to washout or mutation into lower or NP strains. In cases where ES-to-NP mutation rate is significantly lower than ES cell death and washout rates, the model predicted that ES-to-NP mutation is not a major driver for productivity loss, resulting in kinetic behavior very similar to Figure 6B. Due to higher growth rates, NP cells outcompete high-producing cells; increasing the **dilution rate** accelerates these population dynamics (high-producing cells are outcompeted in less time with higher dilution rates) (Figure 6B,C,F).

Bioreactors often demonstrate nonuniform mixing dynamics, and cells can periodically experience localized heterogenous O_2 conditions (Figures S8–S13 in the supplemental information online). Simulations of a case where dissolved oxygen (DO) oscillates rapidly over time due to nonuniform mixing, causing cells to periodically experience localized regions of very low O_2 [34], demonstrates a lower overall yield (Figure 6D,F). The effects of O_2 limitation via liquid–gas mass transfer limitation were also simulated, demonstrating faster titer loss compared with the base model (Figure 6E,F). O_2 oscillation or limitation worsens culture productivity by greater selection against high-producing cells (Figure 6). Moreover, the presence of intermediate-productivity subpopulation strains (MED, LO) can improve continuous fermentation if they remain competitive in growth: modeled by setting $\mu_{max,LO}$ and $\mu_{max,MED}$ values close to $\mu_{max,NP}$, and $K_{LO_{O_2}}$ and $K_{MED_{O_2}}$ values close to $K_{NP_{O_2}}$ (Figure 7). During laboratory strain development, researchers often focus on selecting the highest-producing strain ('winner'), with less attention given to intermediate strains ('losers') that may offer a better balance between growth and productivity. However, in industrial settings, these intermediate strains can outperform the 'winner' under stress during long-term fermentation, highlighting the principle: 'Losers Take Some'.

Finally, our model compared **growth-associated production** and **non-growth-associated production** in continuous culture. The simulation assumed glucose as the only limiting substrate with a maximum biomass threshold (see modeling equations in the supplemental information online). Figure S3 shows higher dilution rates accelerate subpopulation selection, as slower-growing ESs are outcompeted more quickly by non-producers. Growth-associated production may benefit from high dilution rates, given increased substrate and nutrient input. By contrast, mixed- or non-growth-associated production favors lower dilution rates, allowing high-producing but slow-growing cells to persist longer in the bioreactor. To promote non-growth-associated biosynthesis, two-stage fermentation that separates growth from production offers an alternative strategy for generating products primarily during the stationary phase [40].

Concluding remarks

During scale-up of biomanufacturing processes, titer instability poses a major risk. Factors contributing to this issue are multifaceted and complex, often manifesting only at larger scales. Growth stresses may trigger metabolic shifts and dimorphic behavior in yeast hosts like *Y. lipolytica*. Additionally, the accumulation of mutations during extended fermentation processes can result in heterogeneous phenotypes, favoring competitive growth advantages at the expense of product titer. As a result, strains optimized through design-build-test-learn cycles in the laboratory may lack robustness in industrial settings. Elucidating strain titer robustness under suboptimal bioprocess conditions enables the design and operation of industrial biomanufacturing with greater reliability and improved economic performance. Moreover, continuous fermentation of synthetic biology strains has not yet been implemented on an industrial scale. Continuous fermentation can not only enhance productivity but also provide an effective scale-down method for assessing strain scalability. More continuous bioreactor studies should be performed to clarify

Outstanding questions

How can we engineer genetic circuits to improve strain stability in large-scale continuous fermentations?

Which bioproduction targets benefit most from fermentation in oil-based media?

How can systems biology be applied to identify and correct harmful mutational 'hot spots'?

How can kinetic modeling, biosensors, and precision fermentation be leveraged to extend production longevity?

the relationships among metabolic responses, subpopulation dynamics, and bioreactor conditions [5] (see Outstanding questions). To enable industrial-scale fermentations, two complementary strategies can be pursued: (i) precision fermentations through optimization of medium composition, mixing, bioreactor parameters, and process controls; and (ii) strain engineering to reduce metabolic burdens, integrate genes stably into low-mutation genomic sites, or deploy synthetic circuits that favor growth of producing subpopulations.

STAR★METHODS

Detailed methods are provided in the online version of this paper and include the following:

- KEY RESOURCES TABLE
- EXPERIMENTAL MODEL AND STUDY PARTICIPANT DETAILS
  - Strain and media composition
  - Bioreactor cultivation for 2l continuous fermentation
  - Semi-continuous fermentation in the Ambr250 and Subculturing in shaking flasks
- METHOD DETAILS
  - β-Carotene titer measurement
  - Kinetic modeling of population dynamics
- QUANTIFICATION AND STATISTICAL ANALYSIS
  - Microscopy and proteomics analysis

RESOURCE AVAILABILITY

Lead contact

Requests for further information and resources should be directed to and will be fulfilled by the lead contact, Yinjie J. Tang (yinjie.tang@wustl.edu).

Materials availability

This study did not generate new reagents. This study did not generate new plasmids or microbial strains.

Data and code availability

All data reported in this paper will be shared by the lead contact upon request. The code used in this project has been deposited at https://github.com/xav1002/strain_stability_simulation and is publicly available at https://doi.org/10.5281/zenodo.16595031 as of date of publication. Any additional information required to reanalyze the data reported in this paper is available from the lead contact upon request.

Author contributions

Conceptualization: Y.J.T., M.B. Methodology: A.M.W., M.F.D., K.H.C., D.T., C.K., Y.S. Modeling: V.A.X., Y.J.T. Investigation: A.M.W., M.F.D., P.G., K.R.P. Writing – original draft: A.M.W., V.A.X., Y.J.T. Writing – review and editing: all authors. Visualization: A.M.W., V.A.X., C.K., Y.S., D.R.S., R.L.A. Supervision: Y.J.T., D.T., M.B. Funding acquisition: M.B., Y.J.T., D.T., K.R.P.

Acknowledgments

This work is supported by the US Department of Energy's Agile BioFoundry Consortium (M.B., D.T., K.R.P.) and National Science Foundation under Award Numbers (2320104 and 2330245). The authors would like to acknowledge Charan Muddana and Yuqian Gao for their contributions to data collections and analyses. The graphical abstract was generated with Biorender (https://BioRender.com).

Declaration of interests

The authors declare no competing interests.

Supplemental information

Supplemental information associated with this article can be found online https://doi.org/10.1016/j.tibtech.2025.08.019.

References

1. Czajka, J.J. *et al.* (2020) Mitigation of host cell mutations and regime shift during microbial fermentation: a perspective from flux memory. *Curr. Opin. Biotechnol.* 66, 227–235
2. Du, Y.-H. *et al.* (2022) Optimization and scale-up of fermentation processes driven by models. *Bioengineering* 9, 473
3. Wehrs, M. *et al.* (2019) Engineering robust production microbes for large-scale cultivation. *Trends Microbiol.* 27, 524–537
4. Czajka, J.J. *et al.* (2018) Engineering the oleaginous yeast *Yarrowia lipolytica* to produce the aroma compound β-ionone. *Microb. Cell Factories* 17, 136
5. Xie, D. (2022) Continuous biomanufacturing with microbes — upstream progresses and challenges. *Curr. Opin. Biotechnol.* 78, 102793
6. Rugbjerg, P. *et al.* (2018) Diverse genetic error modes constrain large-scale bio-based production. *Nat. Commun.* 9, 787
7. Rugbjerg, P. and Sommer, M.O.A. (2019) Overcoming genetic heterogeneity in industrial fermentations. *Nat. Biotechnol.* 37, 869–876
8. Grune, T. *et al.* (2010) β-Carotene is an important vitamin A source for humans. *J. Nutr.* 140, 2268S–2285S
9. Madzak, C. (2018) Engineering *Yarrowia lipolytica* for use in biotechnological applications: a review of major achievements and recent innovations. *Mol. Biotechnol.* 60, 621–635
10. Yaguchi, A. *et al.* (2018) Engineering yeast for utilization of alternative feedstocks. *Curr. Opin. Biotechnol.* 53, 122–129
11. Humphrey, A. (1998) Shake flask to fermentor: what have we learned? 14, 3–7
12. Samaras, J.J. *et al.* (2020) Flow, suspension and mixing dynamics in DASGIP bioreactors, Part 2. *AIChE J.* 66, e16999
13. Nadal-Rey, G. *et al.* (2022) Computational fluid dynamics modelling of hydrodynamics, mixing and oxygen transfer in industrial bioreactors with Newtonian broths. *Biochem. Eng. J.* 177, 108265
14. Marx, R. *et al.* (2024) CFD evaluation of hydrophobic feedstock bench-scale fermenters for efficient high agitation volumetric mass transfer. *Biotechnol. J.* 19, 2300384
15. Coleman, S.M. *et al.* (2024) Considerations regarding high oil density bioreactor-scale fermentations of *Yarrowia lipolytica* using CFD modeling and experimental validation. *Biotechnol. J.* 19, e202400506
16. Worland, A.M. *et al.* (2020) Analysis of *Yarrowia lipolytica* growth, catabolism, and terpenoid biosynthesis during utilization of lipid-derived feedstock. *Metab. Eng. Commun.* 11, e00130
17. Shuler, M.L. and Kargi, F. (2002) *Bioprocess Engineering: Basic Concepts*, Prentice Hall
18. Papanikolaou, S. *et al.* (2002) Single cell oil production by *Yarrowia lipolytica* growing on an industrial derivative of animal fat in batch cultures. *Appl. Microbiol. Biotechnol.* 58, 308–312
19. Papanikolaou, S. *et al.* (2003) Accumulation of a cocoa-butter-like lipid by *Yarrowia lipolytica* cultivated on agro-industrial residues. *Curr. Microbiol.* 46, 0124–0130
20. Qin, J. *et al.* (2025) Metabolic engineering of *Yarrowia lipolytica* for conversion of waste cooking oil into omega-3 eicosapentaenoic acid. *ACS Eng. Au* 5, 128–139
21. Li, N. *et al.* (2020) Production and excretion of astaxanthin by engineered *Yarrowia lipolytica* using plant oil as both the carbon source and the biocompatible extractant. *Appl. Microbiol. Biotechnol.* 104, 6977–6989
22. Wang, C. *et al.* (2019) Challenges and tackles in metabolic engineering for microbial production of carotenoids. *Microb. Cell Factories* 18, 55
23. Liu, P. *et al.* (2016) Decreased fluidity of cell membranes causes a metal ion deficiency in recombinant *Saccharomyces cerevisiae* producing carotenoids. *J. Ind. Microbiol. Biotechnol.* 43, 525–535
24. Gao, S. *et al.* (2017) Iterative integration of multiple-copy pathway genes in *Yarrowia lipolytica* for heterologous β-carotene production. *Metab. Eng.* 41, 192–201
25. Worland, A.M. *et al.* (2024) Elucidation of triacylglycerol catabolism in *Yarrowia lipolytica*: how cells balance acetyl-CoA and excess reducing equivalents. *Metab. Eng.* 85, 1–13
26. Roppongi, T. *et al.* (2021) Solubility and mass transfer coefficient of oxygen through gas– and water–lipid interfaces. *J. Food Sci.* 86, 867–873
27. Cuvelier, M.-E. *et al.* (2017) Oxygen solubility measured in aqueous or oily media by a method using a non-invasive sensor. *Food Control* 73, 1466–1473
28. Pias, S.C. (2021) How does oxygen diffuse from capillaries to tissue mitochondria? Barriers and pathways. *J. Physiol.* 599, 1769–1782
29. Pomraning, K.R. *et al.* (2018) Regulation of yeast-to-hyphae transition in *Yarrowia lipolytica*. *mSphere* 3 e00541-18
30. Kawasse, F.M. *et al.* (2003) Morphological analysis of *Yarrowia lipolytica* under stress conditions through image processing. *Bioprocess Biosyst. Eng.* 25, 371–375
31. Deparis, Q. *et al.* (2017) Engineering tolerance to industrially relevant stress factors in yeast cell factories. *FEMS Yeast Res.* 17, fox036
32. Wu, G. *et al.* (2016) Metabolic burden: cornerstones in synthetic biology and metabolic engineering applications. *Trends Biotechnol.* 34, 652–664
33. Pouzet, S. *et al.* (2023) Optogenetic control of beta-carotene bioproduction in yeast across multiple lab-scales. *Front. Bioeng. Biotechnol.* 11, 1085268
34. Nadal-Rey, G. *et al.* (2023) Modelling of industrial-scale bioreactors using the particle lifeline approach. *Biochem. Eng. J.* 198, 108989
35. Leplat, C. *et al.* (2018) Overexpression screen reveals transcription factors involved in lipid accumulation in *Yarrowia lipolytica*. *FEMS Yeast Res.* 18, foy037
36. Sleight, S.C. *et al.* (2010) Designing and engineering evolutionary robust genetic circuits. *J. Biol. Eng.* 4, 12
37. Ingram, D. and Stan, G.-B. (2023) Modelling genetic stability in engineered cell populations. *Nat. Commun.* 14, 3471
38. Nuismer, S.L. *et al.* (2021) Methods for measuring the evolutionary stability of engineered genomes to improve their longevity. *Synth. Biol.* 6, ysab018
39. Der, R. *et al.* (2011) Generalized population models and the nature of genetic drift. *Theor. Popul. Biol.* 80, 80–99
40. Chen, G.-Q. and Page, W.J. (1997) Production of poly-b-hydroxybutyrate by *Azotobacter vinelandii* in a two-stage fermentation process. *Biotechnol. Tech.* 11, 347–350
41. Larroude, M. *et al.* (2018) A synthetic biology approach to transform *Yarrowia lipolytica* into a competitive biotechnological producer of β-carotene. *Biotechnol. Bioeng.* 115, 464–472
42. Wu, Z. *et al.* (2024) Population dynamics of engineered microbes under metabolic stress and reward in batch and continuous reactors. *Chem. Eng. J.* 502, 158049
43. Van Riel, M. *et al.* (1983) Fluorescence excitation profiles of beta-carotene in solution and in lipid/water mixtures. *Biochem. Biophys. Res. Commun.* 113, 102–107
44. Pomraning, K.R. *et al.* (2021) Integration of proteomics and metabolomics into the design, build, test, learn cycle to improve 3-hydroxypropionic acid production in *Aspergillus pseudoterreus*. *Front. Bioeng. Biotechnol.* 9, 603832

STAR★METHODS

KEY RESOURCES TABLE

Reagent or resource	Source	Identifier
Chemicals, peptides, and recombinant proteins		
Yeast Peptone Dextrose Growth Media	Millipore Sigma, consisting of yeast extract (1%), peptone (2%) and dextrose (2%) (see EXPERIMENTAL MODEL AND STUDY PARTICIPANT DETAILS)	Yeast Extract CAS Number: 8013-01-2 Yeast Peptone Product Number: 68707 Dextrose CAS Number: 50-99-7
Yeast Peptone Oil Growth Media	Millipore Sigma, consisting of yeast extract (1%), peptone (2%) and canola oil (see EXPERIMENTAL MODEL AND STUDY PARTICIPANT DETAILS)	Yeast Extract CAS Number: 8013-01-2 Yeast Peptone Product Number: 68707 Canola Oil CAS Number: 120962-03-0
Experimental models: organisms/strains		
Yarrowia lipolytica β-carotene strain	Produced by Arch Innotek, St. Louis, USA [4]	N/A
Software and algorithms		
MATLAB	Mathworks	SCR_001622
Original kinetic modeling code	https://doi.org/10.5281/zenodo.16595031	N/A
Other		
2L BIOSTAT B	Sartorius, Germany	N/A
Ambr250	Sartorius, Germany	N/A

EXPERIMENTAL MODEL AND STUDY PARTICIPANT DETAILS

Strain and media composition

The β-carotene producing *Y. lipolytica* strain is a gift from Arch Innotek, St. Louis, USA [4]. Briefly, the mevalonate pathway was optimized by overexpressing eight native genes (*ACAT*, *NphT7*, *HMGS*, *tHMGR*, *MK*, *PMK*, *MPD*, *IPI*, *FPPS*, and *GGPPS*, see abbreviations) to push flux towards acetyl-CoA production and terpene synthesis. Additionally, two heterologous genes (*carB* and *carRP* of *M. circinelloides*) were introduced via random genome integration at the zeta locus to pull flux from GGPP to β-carotene. This engineered yeast shows mixed-growth-associated β-carotene synthesis. Fermentations utilized rich media containing either glucose or oil as a carbon source: YPD (10 g/l yeast extract, 20 g/l peptone, 20 g/l glucose) or YPO (10 g/l yeast extract, 20 g/l peptone, 20 g/l canola oil). One experiment utilized yeast nitrogen base medium with full amino acid supplementation, a defined medium (YNBaa: 1.7 g/l yeast nitrogen base, 5 g/l ammonium sulfate, 2 g/l complete amino acid drop-out mix) with 20 g/l glucose. Yeast extract and peptone were purchased from BD Biosciences (Franklin Lakes, USA). Canola oil was purchased from Schnucks (St. Louis, USA). All other chemicals were purchased from Sigma Aldrich (St. Louis, USA). For all experiments, the engineered strain was recovered from a glycerol stock stored at –80°C onto a YPD agar plate and incubated at 30°C. From the plate, 3–5 red colonies were selected and inoculated into a 20 ml seed culture (with the respective experimental media) and cultured at 250 rpm and 30°C until reaching late exponential phase. The seed culture was used to inoculate experimentation reactors. Additionally, microscope images (e.g., Figure S1 in the supplemental infomration online) were taken to observe cells and post-selection colony resequencing acted as authentication of the purity of the cultures in this study.

Bioreactor cultivation for 2l continuous fermentation

Fermentations were conducted at the Advanced Biofuels and Bioproducts Process Development Unit at Lawrence Berkeley National Laboratory. Fermentations were conducted in 2l bioreactors (BIOSTAT B, Sartorius, Germany). Base process parameters were controlled at culture temperature at 30°C and pH 6.5, maintained at 6.5 by automated addition of 10N NaOH and 10% H_2SO_4. DO was controlled at a setpoint 20%, maintained with constant airflow at 1 vvm and feedback-controlled agitation in the range of 300–1000 rpm. As needed, antifoam was added to control foaming in the bioreactor. For O_2 limited experiments, the DO setpoint was lowered to 10%, with airflow at

0.5 vvm (volume of sparged air to volume of liquid per minute). The bioreactors were initially charged with 1.5 l of the experimental medium. Reactors were inoculated at a target OD_{600} between 0.1 and 0.2 and cultivated in batch mode for the exponential phase. Batch conditions were conducted with base process parameters as described. Continuous cultivation was initiated once 80% of carbon substrate was consumed and biomass reached OD_{600} = 20, typically around 30 hours after inoculation. Continuous cultivation was conducted, with the feed media identical to the batch media, by using automated pump feedback controls. For glucose cultures, residual glucose concentrations were determined via HPLC. An in-house LabView software remotely controlled analog peristaltic pumps (Watson-Marlow 120U) in response to the measured difference between feed input and drain output to maintain reactor volume, ensuring steady-state fermentations. Feed and drain bottles were housed on bench scales (Ohaus Ranger 3000). Ethernet multifunction DAQ devices (LabJack T4) were used to convert digital signals to voltage analog inputs to regulate controls of peristaltic pumps. Silicone tubing connected feed and drain bottles to the reactors. Tubing and bottles were periodically exchanged for sterile replacements to prevent clogs from biomass buildup. The feed media was the same as the batch media. 2l fermentations were conducted with different dilution rates. Filamentous cell formation was observed in the late fermentation stage (Figure S1) and bioreactor conditions (such as oxygen and foaming) were not strictly constant (i.e., not achieving chemostat). Cell morphology was imaged using a microscope (Zeiss Axio Observer ZI, Germany).

Semi-continuous fermentation in the Ambr250 and Subculturing in shaking flasks

We utilized the Ambr® 250 (Sartorius, Germany) multi-parallel bioreactor system to conduct semi-continuous fermentations with different growth mediums (Figure S2 in the supplemental infomration online). In these experiments, cultures were continuously fed at a set dilution rate (0.02 h^{-1} for low O_2 conditions, and 0.04 h^{-1} for all other experiments) and were drained when the reactors reached a 25% increase from the starting volume. Draining was performed automatically via robotic pipette control in the Ambr250 system. Reactors were initially charged with 150 ml batch medium and inoculated at a target OD_{600} between 0.15 and 0.2. The cultures were maintained at the same process parameters as used in 2l fermentations. Semi-continuous cultivation was also initiated after cultures reached late exponential phase. Polypropylene Glycol or antifoam B emulsion (Sigma-Aldrich, St. Louis) was used to control foaming as needed.

Strain stability is often evaluated via successive passaging in shake flasks. This method is favored for its simplicity, cost-effectiveness, and high-throughput potential. Shake flask passaging experiments were conducted with YPD and YPO at 30°C and 250 rpm (triplicates, $n = 3$), as shown in our past study [4]. Specifically, cultures were inoculated into 50 ml media in a 250 ml non-baffled flask at 1% v/v (initial $OD_{600} < 0.1$). Subcultures were performed every 24 hours after cells had ~7 generations to reach an OD_{600} above 5. All subcultures were maintained for 72 hours to allow for prolonged production phase before harvesting for β-carotene analysis. In summary, 10 passages were conducted for YPD cultures, and 15 passages were conducted for YPO cultures, reaching ~75 and ~110 generations, respectively. YPD-grown cultures lost nearly all production after 10 passages, while YPO-grown cultures maintained >60% of productivity even after 15 passages.

Finally, this study defined growth generations (gens) as: $2^{gens} = \frac{Final\ Biomass}{Initial\ Biomass}$. For batch culture or shake flask culture: $gens = \frac{\ln\left(\frac{Final\ biomass}{Initial\ biomasss}\right)}{\ln(2)}$. Continuous culture with dilution rate (D) and cultivation time (Δt): $gens = \frac{D\ \Delta t}{ln(2)}$. For Ambr system, a simplified equation estimates: $gens = \frac{\ln\left[\frac{total\ biomass\ harvested}{initial\ biomass\ in\ bioreactor}\right]}{\ln(2)}$.

METHOD DETAILS

β-Carotene titer measurement

β-Carotene titer was quantified via a spectrophotometry method [41]. Briefly, cell pellets were collected from the fermentation broth and combined with acid-washed glass beads (425–600 μm diameter) in a microcentrifuge tube. To this, an extraction solution comprising of 1:1 (v/v) hexane, ethyl acetate, and 0.1% butylated hydroxytoluene (BHT) was added. The mixture was agitated with a vortex mixer until the cell pellets were fully disrupted with no visible orange coloration remaining. Lysed cells were pelleted, and the concentration of the extracted β-carotene solution was determined via spectrophotometry from absorbance at 452 nm with a standard curve of β-carotene standard (Sigma Aldrich, St. Louis, MO). β-Carotene concentration was confirmed via HPLC utilizing an Agilent Technologies 1200 Infinity Series HPLC equipped with a UV-VIS detector (450 nm) and a C18 column (4.6 × 150 mm). The mobile phase comprised of 7:3 (v/v) methanol and acetonitrile ran at a flow rate of 1.5 ml/min and 40°C.

Kinetic modeling of population dynamics

Kinetic modeling provides a framework to explain the effect of heterogeneous population on bio-productions [42]. Our model simulates varying levels of β-carotene producers, denoted as X_i, where i = HI (high), MED (medium), and LO (low), alongside non-producing strains, represented as X_{NP} (Equations 1 and 2). Yeast growth (X_i) is a function of glucose (G) and averaged DO (O_2) concentration; the Monod equation is used to represent the limitation effect of these two substrates on biomass growth. The glucose and DO concentrations are represented by Equations 3 and 4, respectively. The cosine term in Equation 4 is a simplified approach to simulate DO oscillations when cells circulate within poorly mixed bioreactors (Figure S5 in the supplemental infomration online). The parameter A (g l^{-1} h^{-1}) represents the amplitude of the DO oscillations experienced by the cells and is chosen to yield a reasonable oxygen oscillation (maximum DO near oxygen solubility limit and minimum DO near zero); the parameter ω represents the angular frequency of DO oscillations experienced by cells and is linked to the bioreactor mixing conditions. β-Carotene (P) synthesis is assumed to be mixed growth associated (Equation 5). The model explores both continuous and sub-cultured batch fermentations by using MATLAB ODE Suite (MathWorks, USA).

$$\frac{dX_i}{dt} = X_i\left[\mu_{max,i}\left(\frac{G}{K_{i_G}+G}\right)\left(\frac{O_2}{K_{i_{O_2}}+O_2}\right) - k_{d_i} - M_{R_i}\mu_{max,i}\left(\frac{G}{K_{i_G}+G}\right)\left(\frac{O_2}{K_{i_{O_2}}+O_2}\right) - D\right] \quad [1]$$

$$\frac{dX_{NP}}{dt} = X_{NP}\left[\mu_{max,NP}\left(\frac{G}{K_{NP_G}+G}\right)\left(\frac{O_2}{K_{NP_{O_2}}+O_2}\right) - k_{d_i} + \sum M_{R_i}\mu_{max,i}\left(\frac{G}{K_{i_G}+G}\right)\left(\frac{O_2}{K_{i_{O_2}}+O_2}\right) - D\right] \quad [2]$$

$$\frac{dG}{dt} = D(G_{in} - G) - Y_{NP_G}X_{NP}\mu_{max,NP}\left(\frac{G}{K_{NP_G}+G}\right)\left(\frac{O_2}{K_{NP_{O_2}}+O_2}\right) + \sum -Y_{i_G}X_i\mu_{max,i}\left(\frac{G}{K_{i_G}+G}\right)\left(\frac{O_2}{K_{i_{O_2}}+O_2}\right) \quad [3]$$

$$\frac{dO_2}{dt} = k_La\left(O_2^* - O_2\right) + A\cos\left(\omega\frac{\pi t}{2}\right) - Y_{NP_{O_2}}X_{NP}\mu_{max,NP}\left(\frac{G}{K_{NP_G}+G}\right)\left(\frac{O_2}{K_{NP_{O_2}}+O_2}\right) + \sum -Y_{i_{O_2}}X_i\mu_{max,i}\left(\frac{G}{K_{i_G}+G}\right)\left(\frac{O_2}{K_{i_{O_2}}+O_2}\right) \quad [4]$$

$$\frac{dP}{dt} = -DP + \sum X_i\left[\alpha_{i_P}\mu_{max,i}\left(\frac{G}{K_{i_G}+G}\right)\left(\frac{O_2}{K_{i_{O_2}}+O_2}\right) + \beta_{i_P}\right] \quad [5]$$

Here, $\mu_{max,i}$ is the maximum specific growth rate for yeast strain i (h^{-1}); K_{i_G} and $K_{i_{O_2}}$ are the half-saturation concentration of glucose and averaged DO (respectively) with respect to the growth of yeast strain i (g l^{-1}). For higher producing subpopulations, the model decreases $\mu_{max,i}$ and increases $K_{i_{O_2}}$ to simulate slower growth rates and greater sensitivity to oxygen limitation stresses. k_{d_i} is the specific cell death rate of yeast strain i (h^{-1}); M_{R_i} is the specific mutation rate of yeast strain i (unitless); D is the dilution rate of the bioreactor system (h^{-1}); G_{in} is the inlet glucose concentration (g l^{-1}); Y_{i_G} and $Y_{i_{O_2}}$ are the yield coefficients of yeast strain i with respect to glucose (g-biomass g^{-1}-glucose) and average DO (g-biomass g^{-1}-oxygen), respectively; k_La is the volumetric mass transfer coefficient for O_2 (h^{-1}); O_2 is the solubility of O_2 (g l^{-1}). Since β-carotene titers are only at the level of mg/l, the glucose consumption for β-carotene synthesis was neglected. For further details, see Table S1 and Figures S3–S8 in the supplemental information online. As noted, these growth rate coefficients were assumed to qualitatively explain the observed fermentation behavior, not to quantitatively fit the experimental data.

QUANTIFICATION AND STATISTICAL ANALYSIS

Microscopy and proteomics analysis

We quantified β-carotene levels within single cells by detecting β-carotene autofluorescence at 480–520 nm when excited with blue light [43]. Samples were collected throughout the fermentation and frozen as pellets at –80°C for later analysis. Cell pellets were thawed, then resuspended in 200 µl PBS and stained for 5 minutes using calcofluor white to highlight cell walls. Images were acquired using a Nikon Ti2 widefield microscope fitted with a Prime BSI sCMOS camera (Teledyne Technologies, USA). Calcofluor white was imaged with blue fluorescence filters and β-carotene was imaged using green fluorescence filters. Light intensity and

exposure times were kept constant across samples. Twenty-one Z-stacks were taken per image for a total depth of 7 μm. Image preparation and analysis was performed using ImageJ/FIJI. Quantification of cell circularity was determined based on area and perimeter of cells. Significance was calculated using a Students *t*-test (n.s. = $P > 0.05$, *** = $P < 0.001$).

We performed proteomics analysis of continuous bioreactor samples at Pacific Northwest National Laboratory (https://www.emsl.pnnl.gov/). Sample preparation, instrument acquisition and data analysis were performed as previously reported [44]. In brief, global and targeted proteomics was performed as in previously established LC-MS/MS methods and data analysis workflows except slight adjustments to the mass spectrometry acquisition settings in global proteomics. In global proteomics, peptide digests were analyzed using a Q Exactive HF-X mass spectrometer (Thermo Fisher Scientific, USA) in data-dependent acquisition mode. Mass spectrometer settings were as following: full MS (AGC, 3 × 106; resolution, 60 000; m/z range, 300–1800; maximum ion time, 20 ms); MS/MS (AGC, 1 × 105; resolution, 30 000; m/z range, 200–2000; maximum ion time, 100 ms; TopN, 12; isolation width, 0.7 Da; dynamic exclusion, 45.0 s; collision energy, NCE 30). The analysis used volcano plot to illustrate differentially abundant proteins.